



Discrimination of Crop and Weeds on Visible and Visible/Near-Infrared Spectrums Using Support Vector Machine, Artificial Neural Network and Decision Tree

^{1,3} Wei Deng, ² Yanbo Huang, ^{1,3} Chunjiang Zhao, ^{1,3} Xiu Wang

¹ Beijing Research Center of Intelligent Equipment for Agriculture, Beijing Academy of Agriculture and forestry Science, Beijing 100097, China

² United States Department of Agriculture, Agricultural Research Service, Crop Production Systems Research Unit, Stoneville, Mississippi, USA

³ National Research Center of Intelligent Equipment for Agriculture, Beijing 100097, China

¹ Tel.: +8610 51503346, fax: +8610 51503750

¹ E-mail: dengw@nercita.org.cn

Received: 19 November 2013 /Accepted: 27 December 2013 /Published: 14 March 2014

Abstract: Weeds are regarded as farmers' natural enemy. In order to avoid excessive pesticide residues, the destruction of ecological environment, and to guarantee the quality and safety of agricultural products, it is urgent to develop highly-efficient weed management methods. Amongst, weed discrimination is the key part. There have been a lot of researches on weed detection/discrimination using spectral measurement on plant leaf/canopy. However, as reported so far the spectral ranges from the researches were not consistent and no research was reported to determine more efficient wavelength range for weed classification. Some researchers adopted visible spectrum, some adopted near-infrared spectrum, the others adopted both visible and near-infrared spectrum. The purpose of this study was to compare the classifications of the spectral reflectance in range of 350 ~ 760 nm and in 350 ~ 2500 nm for crop/weed discrimination. Through spectral analysis of these data respectively using three kinds of modeling methods of Support Vector Machines (SVMs), Artificial Neural Network (ANN), and Decision Tree (DT), the results showed that the three classifiers could differentiate crop and weeds better in 350 ~ 760 nm wavelength range than in 350 ~ 2500 nm. Therefore, the visible wavelength range could be good enough to meet the requirement for crop/weed spectral discrimination, which might reduce the cost of weed detect sensors. Copyright © 2014 IFSA Publishing, S. L.

Keywords: Crop/weed discrimination, Spectral analysis, Visible and near-infrared spectrum, Wavelength range.

1. Introduction

According to the research report from the United Nations Food and Agriculture Organization (FAO) in August 2009, weeds should be regarded as farmers' No. 1 natural enemy. The report said that

according to a leading environmental research organization, Land Care of New Zealand, weeds cause about \$ 95 billion every year in the lost food production at global level, compared with \$ 85 billion for pathogens, \$ 46 billion for insects and \$ 2.4 billion for vertebrates (excluding humans).

Of the \$ 95 billion, \$ 70 billion are estimated to be lost in developing countries [1]. In China, the crop yield losses annually caused by weeds sum up to about 10 % of the gross grain output [2]. Facing the severity of the crop loses caused by weeds, it is urgent for us to seek highly efficient methods for effective weed control. The chemical weeding method commonly adopted at present has provoked a lot of problems, such as excessive pesticide residues, growing number of pesticide-resistant weeds, destruction of the ecological environment, and quality and safety of agricultural products [3]. Therefore, people have gradually realized that it is critical to have a method which could not only control the growth of weeds, but also decrease the use of herbicides, and hence prevent from excessive herbicide application.

There are many techniques which could be used for weed detection, such as, photoelectric, ultrasonic [4, 5], microwave [6, 7], and image processing [8, 9] detection techniques. The microwave technique is not subject to the effects of heat, noise, humidity, airflow and dust, and is suitable for harsh environments because of its anti-jamming ability. However, this technique is still not suitable for agriculture due to the restriction of the complexity of communication and control techniques and being less cost-effective. The image processing technique can detect the target's profile and determine the coverage and amount of spraying, but most usage of this technique is still at the laboratory stage and seldom applied in real-time detection in fields because of its poor stability, large amount of data processing, relatively slow response, and the higher costs. In comparison with other detection techniques, spectral technology has been widely used in real-time detection system because of its fast response, availability for non-contact detection, strong anti-interference, high reliability, low cost, simple and small configuration, and low power consumption [10, 11]. The method of discriminating crop and weeds using spectral features could be realized for real-time detection. Therefore, it is necessary to conduct more studies on spectral detection and classification of weeds and crops.

Brown et al. [12] measured the reflectance of a number of weeds in the spectral range of 400 ~ 900 nm in cotton fields. In order to differentiate cotton and weeds, four characteristic wavelengths, 440, 530, 650 and 730 nm, were determined. Vrindts et al. [13] measured reflectance of potato, sugar beet, maize and various weeds and soil in the range of 200 ~ 2000 nm. Analysis results showed that two wavelengths, 1715 and 1925 nm, could be used for classifying sugar beet, weeds and soil, three wavelengths, 645, 695 and 1085 nm for corn and weeds, and three other wavelengths, 515, 765 and 1935 nm for potatoes, weeds and soil. Borregaard et al [14] measured the reflectance of potatoes, beet, and several weeds within the waveband range of 670 ~ 1070 nm using an imaging spectrometer. Through analysis using the selected

characteristic wavelengths, the recognition rate of potato and weeds was 94 % and that of sugar beet and weeds was 87 %. Jurado-Exposito et al. [15] studied the method of distinguishing seven kinds of broadleaf weeds, sunflower and wheat seedlings, and found that 750 ~ 950 nm near-infrared spectrum could be used to distinguish. Prasad et al [16] studied how to select the optimal wavebands within the spectral range of 400 ~ 2500 nm in order to correctly classify plants (shrubs, weeds) and crops (maize). Through modeling and analyzing, the results showed that the prediction accuracy can reach 90 %. Mao Wenhua et al. [17] measured the spectral reflectance of wheat, goosefoots, shepherd's purse, and other several weeds within the spectral waveband range of 700 ~ 1100 nm. The results of discriminant analysis showed that the correct classification rate was 97 % when the characteristic wavelengths were used to establish the discrimination model. Zhu et al [18] classified three weeds (goose grass, Alternanthera philoxeroides, Amaranthus ascendens) and soybean seedlings using the spectral reflectance within 325 ~ 1075 nm wavebands. The results showed that it is feasible to utilize the visible / near-infrared spectral information to identify soybean seedlings and the three kinds of accompanied weeds. Deng et al [19] collected the spectral reflectance of plant canopy of corn, crabgrass, and barnyard grass in spectral range of 350 ~ 2500 nm in fields. After modeling the measured data, the results showed that the correct identification rate was 80 %. Chen et al [20] measured the spectral reflectance of rice, cotton, barnyard grass, and Cephalanoplos in the laboratory using a spectrometer with the spectral range of 350 ~ 2500 nm. By modeling using the extracted characteristic wavelengths, the analysis results showed that monocotyledons, like rice and barnyard grass, can be accurately classified using 5 characteristic wavelengths, 375, 465, 585, 705, and 1035 nm. The correct classification rate was 100 %. Liu et al [21] acquired the hyperspectral data of carrot seedlings and several wild weeds, like goose grass, humifuse euphorbia herb, and Portulaca oleracea L., in the spectral range of 380 ~ 760 nm using a ground imaging spectroscopy system. The analysis results showed that the classification rate was up to 91 % when all the weeds were viewed as a whole class and was 85% when each weed was separately viewed as a class. Zu et al [22] acquired the canopy spectral reflectance of two kinds of cabbages and five kinds of weeds (barnyard grass, setaria, crabgrass, goosegrass, and pigweed) within 350 ~ 2500 nm wavelength band using a spectrometer. After data preprocessing and classification modeling, the analysis results indicated that 100 % correct classification rate could be achieved.

From the studies above, it could be seen that (1) due to the difference of measuring instruments, measuring environmental conditions, measurement range, and the target of study, the characteristic wavelengths selected were completely different. As a

result, it will be difficult to develop a standard and generic system for weed recognition and classification. (2) The spectral ranges determined and used in the previous researches were not consistent, which might be because the existing measuring instruments they used in the studies were different. Some researchers adopted visible spectrum, some adopted near-infrared spectrum, the others adopted both visible and near-infrared spectrum. Meanwhile, with the development of spectroscopy technology, it is widely considered that the wider the spectral wavelength range is, the more information and the higher correct classification rate we could acquire. However, the wider the wavelength range is, the more expensive the measuring instrument will be. Further, there has been no exact evidence showing that we could obtain higher correct classification rate of crop and weeds from the wider spectral reflectance. Therefore, this study is to compare the effect of different measuring wavebands for classification of crops and weeds. The specific research objective is to compare the correct classification rates separately obtained from the reflectance data of 350 ~ 760 nm visible wavelength range and the data of 350 ~ 2500 nm visible and near-infrared (VNIR) wavelength range, respectively using the classifiers of Support Vector Machines (SVMs), Artificial Neural Network (ANN), and Decision Tree (DT).

2. Materials and Methods

2.1. Experimental Equipment

The spectral data of the plants were measured using a handheld FieldSpec 3 spectroradiometer (ASD, Boulder, Colorado, USA) in the field. The measuring range of the spectroradiometer is 350 ~ 2500 nm, within which the spectral resolution is 3 nm in the range of 350 ~ 1000 nm and 10 nm in the range of 1000 ~ 2500 nm. The sampling interval is 1nm, that is, to obtain a measured datum every 1nm. The measuring procedure was arranged as to measure the reflection energy of the white reference board (I_s), and then to measure the reflection energy of the plant (I_r). With the known reflectivity (R_r) of the reference board, the spectral reflectivity (R_s) of the measured object can be calculated as follow:

$$R_s = (I_s / I_r) \times R_r \quad (1)$$

2.2. Data Acquisition

Corn and weeds (*Dchinochloa crassgalli*, and *Echinochloa crusgalli*) were selected as research objects which were measured for spectral analysis in this study. The spectral data were respectively obtained at the growth periods of three weeks and six

weeks after the emergence of corn and weeds seedlings. The measurements in fields were conducted during sunny days between 11:00 am to 14:00 pm and all the data were collected in the experimental fields of China Agricultural University on May, 24th, and June, 21st, 2008.

2.3. Observation and Sampling of Spectral Data

In order to reduce the random error from the measurement, each plant measurement was repeated 5 times successively to produce an average value. A typical measured spectrum curve of the plants for the study and its spectral reflectivity curve are separately shown in Fig. 1. There are many burrs observed on the reflectivity curve of Fig. 1 (b) after 1800 nm which should be caused by noise. The same effect of noise also indicates between 1300 and 1400 nm. As a result, the wavelength range was selected as 350 ~ 1300 nm and 1400 ~ 1800 nm for data classification modeling. Because the sampling interval is 1 nm, the sampling dimensional number of each spectral curve is 1352.

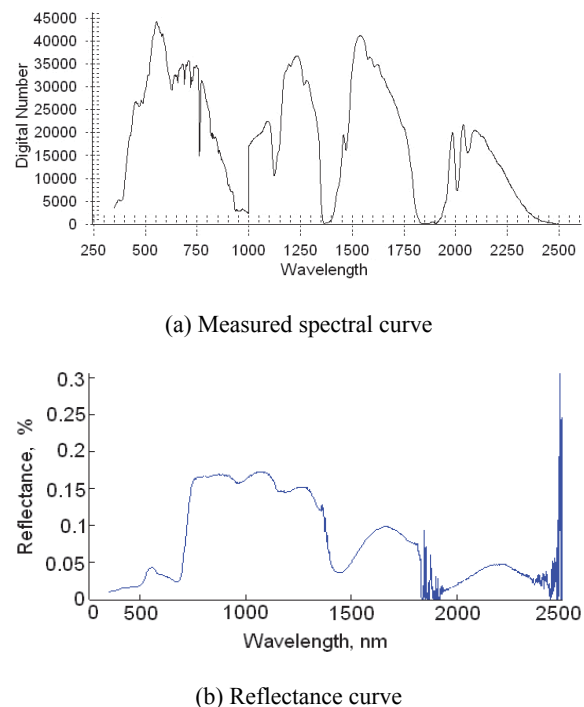


Fig. 1. Measured spectral curve and corresponding reflectance curve.

In order to verify if there is any difference between the correct classification rates when modeling using the spectral reflectance based on visible and VNIR spectrum, the measured spectral data were arranged into two wavelength ranges, namely 350 ~ 760 nm and 350 ~ 2500 nm, for the reason that visible light wavelength normally refers to as the range 350 ~ 760 nm and near-infrared

(NIR) wavelength range is $760 \sim 2500$ nm. For the model in the $350 \sim 760$ nm wavelength range, the sampling dimensional number of each spectral curve is 410, and for the model in $350 \sim 2500$ nm, the sampling dimensional number of each spectral curve is 1352.

2.4. Measured Data

The sample data contained 48 corn samples (category 1), 33 *Echinochloa crusgalli* samples (category 2), and 33 *Dchinochloa crasgalli* samples (category 3), respectively. From the sample data, 32 corn samples, 22 *Echinochloa crusgalli* samples, and 22 *Dchinochloa crasgalli* samples were used for classification model training. While, 16 corn samples, 11 *Echinochloa crusgalli* samples and 11 *Dchinochloa crasgalli* samples were used for classification model testing sample. Therefore, the total number of the sample data is 76 and 38 for model training and testing, respectively.

2.5. Modeling Computing

2.5.1. SVMs Classifier

In machine learning, SVMs are supervised learning models with associated learning algorithms that analyze data and recognize patterns, used for classification and regression analysis. The basic SVM takes a set of input data and predicts, for each given input, which of two possible classes forms the output, making it a non-probabilistic binary linear classifier. Given a set of training examples, each marked as belonging to one of two categories, an SVM training algorithm builds a model that assigns new examples into one category or the other. An SVM model is a representation of the examples as points in space, mapped so that the examples of the separate categories are divided by a clear gap that is as wide as possible. New examples are then mapped into that same space and predicted to belong to a category based on which side of the gap they fall on. In addition to performing linear classification, SVMs can efficiently perform a non-linear classification using what is called the kernel trick, implicitly mapping their inputs into high-dimensional feature spaces [23].

More formally, suppose that the linearly divisible sample set is (x_i, y_i) and the regimentation tab is $i = 1, \dots, n$; $y = \{+1, -1\}$. This classification is to find the optimal hyper-plane $w \cdot x + b = 0$, so that the sample set can be correctly and absolutely separated and the distance of the nearest two classification points in the hyper-plane is the maximum as shown in Fig. 2.

Normalizing the hyper-plane equation and making the classification interval to be $2/\|w\|$, we can find that if we want to maximize the interval,

we will minimize $\|w\|^2$, meanwhile, for all the subscript i that can make $y_i = 1$, there exists $w \cdot x_i + b \geq 1$, for all subscript i that can make $y_i = -1$, there exists $w \cdot x^i + b \leq -1$. Therefore, if you want to search for the optimal hyper-plane classification, you must solve the following equation:

$$\min \|w\|^2 / 2, \quad (2)$$

$$s.t. y_i \cdot \langle w \cdot x + b \rangle \geq 1, i=1, 2, \dots, n$$

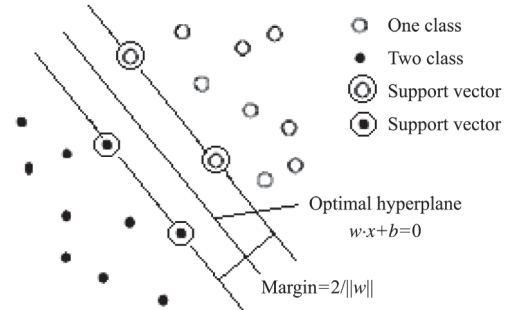


Fig. 2. Schematic of optimal hyperplane.

This equation can be solved by evaluating the saddle point of the Lagrange Function. Generally, we should solve the following duality formula according to Lagrangian duality theory:

$$\max \sum_{i=1}^n a_i - \frac{1}{2} \sum_{i=1}^n \sum_{j=1}^n a_i a_j y_i y_j \langle X_i \cdot X_j \rangle, \quad (3)$$

$$s.t. \sum_{i=1}^n a_i y_i = 0, a_i \geq 0, i=1, \dots, n$$

If you can get the optimal solution a^* , you can also get the following formula that constructs the hyper-plane:

$$W^* = \sum_{i=1}^n y_i a_i^* X_i,$$

$$b^* = y_i - \sum_{i=1}^n y_i a_i^* (X_i \cdot X_j), \quad (4)$$

where X_i and X_j are the support vector (SV) of the two classification, and the points are the few sample points that are closest to the hyper-plane whose a_i is non-zero [24].

The classification results may vary when different kernel functions are used to model the same data samples. The combination of the 3rd order polynomial kernel function in a SVM and one-on-one multi-classification could be used to build the three-category model to classify corn, *Dchinochloa crasgalli*, and *Echinochloa crusgalli* [19]. Specifically, one-on-one multi-classification is a voting method by which the category that got the most votes should be determined as the correct

category. Taking the case of SVM classifier as an example, the data $X_{i,j}$ which is one of the measured spectral samples (where, ‘ i ’ is the category number, ‘ j ’ is the sequence number in each category) in Table 1 can be classified using three SVM bi-classification models. Then all the 38 testing sample will be tested using the three bi-classification models and result in 3 groups of bi-classifying results (shown as the example in Table 4 and Table 5, Column (2), (3), and (4)). After voting for the bi-classifying results (Column (2), (3), and (4)) using the one-on-one multi-classification method, the category that has the most votes should be the category of $X_{i,j}$.

The SVM classification model was programmed using the MATLAB functions built in MATLAB version 7 (MathWorks, Natick, Massachusetts, USA). The MATLAB functions used are:

```
SVMstruct=svmtrain (train, group)
Class=svmclassify (SVMstruct, test)
```

The resulting SVM classification model is outputted in the variable ‘SVMstruct’. The ‘svmtrain’ function calibrates the SVM classification model. The model is then used to classify the test sample data using another function ‘svmclassify’. ‘Train’ stores the training sample data and ‘group’ is the output of the training sample data. In the MATLAB program, the category is coded as 1, 5, and 10 for category 1, category 2 and category 3, respectively. The structures of the bi-classification models of category 1 and category 2, category 2 and category 3, and category 1 and category 3 are separately configured.

The training data format is shown in Table 1.

Table 1. Data format of the training samples for three SVM bi-classifications.

Bi-classification for category 1 and 2 (Column 1)		Bi-classification for category 2 and 3 (Column 2)		Bi-classification for category 1 and 3 (Column 3)	
Input ($X_{i,j}$)	Output	Input ($X_{i,j}$)	Output	Input ($X_{i,j}$)	Output
$X_{1,1}$	1	$X_{2,1}$	5	$X_{1,1}$	1
$X_{1,2}$	1	$X_{2,2}$	5	$X_{1,2}$	1
:	:	:	:	:	:
$X_{1,32}$	1	$X_{2,22}$	5	$X_{1,32}$	1
$X_{2,1}$	5	$X_{3,1}$	10	$X_{3,1}$	10
$X_{2,2}$	5	$X_{3,2}$	10	$X_{3,2}$	10
:	:	:	:	:	:
$X_{2,22}$	5	$X_{3,22}$	10	$X_{3,22}$	10

For the model of 350 ~ 2500 nm, the training samples were a 1352×54 matrix for bi-classification of category 1 and 2 (See the Column 1 in Table 1), a 1352×44 matrix for bi-classification of category 2 and 3 (See the Column 2 in Table 1), and a 1352×54

matrix for bi-classification of category 1 and 3 (See the Column 3 in Table 1), respectively. The testing samples were a 1352×27 matrix for category 1 and 2, a 1352×11 matrix for category 2 and 3, and a 1352×27 matrix for category 1 and 3, respectively. Similarly, for the model of 350 ~ 760 nm, the training samples were a 410×54 matrix for bi-classification of category 1 and 2 (See the Column 1 in Table 1), a 410×44 matrix for bi-classification of category 2 and 3 (See the Column 2 in Table 1), and a 410×54 matrix for bi-classification of category 1 and 3 (See the Column 3 in Table 1), respectively. The testing samples were a 410×27 matrix for category 1 and 2, a 410×11 matrix for category 2 and 3, and a 410×27 matrix for category 1 and 3, respectively.

2.5.2. RBF-NN Classifier

RBF-NN (Radial Basis Function – Neural Network) uses a RBF as the transfer function for each node in the network’s hidden layer, where the RBF is typically defined as a Gaussian function. It allows the input vectors expand into a high dimensional space and the connection weights is linear to the network output, which adopts a linear optimization algorithm. It also has the capability of approximating to any nonlinear mapping, which can greatly improve the problem of local minimum [25]. Fewer weights need to be adjusted at the input layer to avoid the tedious calculation, local minimum, slow convergence, and other shortcomings in the backpropagation (BP) algorithm for multilayer perceptron (MLP) so that RBF-NN has a fast learning process. Therefore, RBF-NN has better ability compared with BP-MLP in respects of approximating capability, classification capability, and learning speed [26]. The structure diagram of a single-output RBF-NN was shown in Fig. 3. From the principle of ANN, it is straightforward to expand it to the case of multiple-input and multiple-output modeling system.

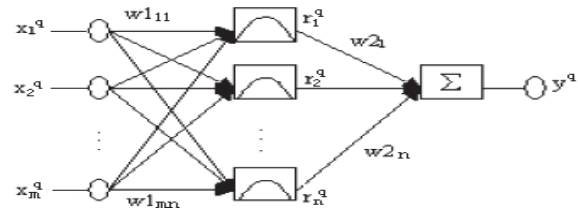


Fig. 3. Structure diagram of RBF-NN.

In the study, three vectors, (1 0 0), (0 1 0), and (0 0 1), were respectively assigned to corn, Dchinnochloa crassgalli, and Echinochloa crusgalli to represent the standard output for the multiple-input and multiple-output RBF-NN classifier, as shown in Table 2. The RBF-NN model was also programmed

using the MATLAB function in the toolbox of neural networks, shown as follows.

`net = newrb (train, group, spread)`

In the function, ‘train’ and ‘group’ are defined the same as the functions for SVM. Herein, for modeling using the data of 350 ~ 2500 nm, ‘train’ is a 1352×76 matrix, which means a total of 76 samples and 1352 data for each sample; ‘group’ is a 3×76 matrix. For modeling using the data of 350 ~ 760 nm, ‘train’ is a 410×76 matrix, which means a total of 76 samples and 410 data for each sample; ‘group’ is a 3×76 matrix. ‘spread’, the extension parameter of the RBF, whose default value is 1.0, was chosen as 1.5 because of the higher correct classification rate. The test sample data were classified using the function as follows so as to verify the identification ability of the established model.

`Y = sim (net, test)`

where ‘test’ is a 1352×38 matrix for modeling the data of 350 ~ 2500 nm and a 410×38 matrix for modeling the data of 350 ~ 760 nm.

Table 2. Data format of the training samples for ANN.

Data format of the training samples		Data format of the testing samples	
Input ($X_{i,j}$)	Output	Input ($Z_{i,j}$)	Output
$X_{1,1}$	1 0 0	$Z_{1,1}$	1 0 0
$X_{1,2}$	1 0 0	$Z_{1,2}$	1 0 0
:	:	:	:
$X_{1,32}$	1 0 0	$Z_{1,16}$	1 0 0
$X_{2,1}$	0 1 0	$Z_{2,1}$	0 1 0
$X_{2,2}$	0 1 0	$Z_{2,2}$	0 1 0
:	:	:	:
$X_{2,22}$	0 1 0	$Z_{2,11}$	0 1 0
$X_{3,1}$	0 0 1	$Z_{3,1}$	0 0 1
$X_{3,2}$	0 0 1	$Z_{3,2}$	0 0 1
:	:	:	:
$X_{3,22}$	0 0 1	$Z_{3,11}$	0 0 1

2.5.3. DT Classifier

DT is a kind of algorithm with a tree structure which consists of a root node, a series of internal nodes and branches and several leaf nodes (terminal nodes). Each internal node has only one parent node and two or more child nodes. The connections between a parent node and its child nodes form as the branches. Each internal node represents the property needed to be tested in a decision-making process. Each branch represents one of the test results so that different attribute values form different branches; meanwhile, each leaf node represents a category, namely the classification result. Therefore, the highest level of the tree known as the root node is the beginning of the decision tree [27]. The simple diagram for a binary decision tree classifier is shown in Fig. 4, from which the basic components for a DT, root node, node, branch, and leaf nodes are present.

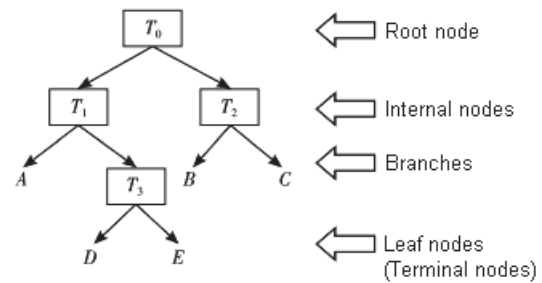


Fig. 4. Structure diagram of a DT.

DT algorithm is a visual representation of knowledge and data mining method, which converts the complex decision-making process into rules or judgments easy to be understood and expressed. DT has many advantages that other algorithms don't have [28]. For example, training speed is fast; non-linear mapping is available even if there is no assumption of the form of data distribution; the process is not a black-box, which can form the classifying rules easy to be understood, and have the ability to complete the built-in feature selection. However, this algorithm needs a larger sample size to achieve a better classification result.

For the study, the category codes, 1, 5, and 10, were allotted to corn, *Dchinochloa crassgalli*, and *Echinochloa crusgalli*, respectively, as the standard output of DT classifier, as shown in Table 3.

Table 3. Data format of the training samples for DT.

Data format of the training samples		Data format of the testing samples	
Input ($X_{i,j}$)	Output	Input ($Z_{i,j}$)	Output
$X_{1,1}$	1	$Z_{1,1}$	1
$X_{1,2}$	1	$Z_{1,2}$	1
:	:	:	:
$X_{1,32}$	1	$Z_{1,16}$	1
$X_{2,1}$	5	$Z_{2,1}$	5
$X_{2,2}$	5	$Z_{2,2}$	5
:	:	:	:
$X_{2,22}$	5	$Z_{2,11}$	5
$X_{3,1}$	10	$Z_{3,1}$	10
$X_{3,2}$	10	$Z_{3,2}$	10
:	:	:	:
$X_{3,22}$	10	$Z_{3,11}$	10

The model was programmed using MATLAB functions, shown as follows:

`treestruct=classregtree (train, group, 'splitmin', 1)
result=eval (treestruct, test)`

Where, ‘treestruct’ is the trained DT model; ‘classregtree’ is the function used to train the sample and set up the DT classification model; ‘eval’ represents the function in which the test sample ‘test’ can be calculated and classified using the established DT model in order to test the classification ability of the model. The data format of ‘train’, ‘group’, and ‘test’ is the same as mentioned in Section 2.5.2.

3. Results and Discussion

The results of SVM, DT and RBF-NN classifiers for classifying corn, Dchinochloa crasgalli, and Echinochloa crusgalli using the spectral data of 350 ~ 2500 nm and 350 ~ 760 nm wavelength ranges are shown in Table 4 and Table 5.

For both tables, Column (2), (3), and (4) respectively show the bi-classification results of category 1&2, category 2 & 3, and category 1 & 3 for SVM classification. The Column (5) displays the results of voting to Column (2), (3), and (4) by using the method of one-on-one multi-classification voting. Through comparing the voting results to the real value (Column (1)), the true judgment of SVM classifier for classifying the testing sample were acquired and shown in Column (6). While, Column (7) exhibits the tri-classification results of the DT

classifier for classifying the testing sample. In the same way, through comparing the tri-classification results DT classifier to the real value (Column (1)), the true judgment of the DT classifier for classifying the testing sample were made and shown in Column (8). Similarly, the tri-classification results of the RBF-NN classifier are shown in Column (9). Through comparing the classification results to the standard vectors (the real value for each sample) (Column (10)), the true judgment of RBF-NN classifier for classifying the testing sample were achieved and displayed in Column (11). For all the judgments in Table 4 and 5, “1” represents “True value”, and “0” is “false”. From the true judgment results of SVM, DT and RBF-NN classifiers in Column (6), (8), and (11), the correct classification rates of the three classifiers are shown at the bottom line in Tables 4 and 5.

Table 4. Classification results of SVM, DT, and ANN using spectral data of 350 ~ 2500 nm (Category 1-corn, Category 2-Dchinochloa crasgalli, and Category 3-Echinochloa crusgalli).

NO	Real Value (1)	SVM Classification					DT Classification		ANN Classification				
		Category 1&2 (2)	Category 2&3 (3)	Category 1&3 (4)	Voting results (5)	True Judgment (6)	Results (7)	True Judgment (8)	Normalized results (9)			Real value (10)	
1	1	1	10	1	1	1	3.2222	0	0.1748	-1	1	1	0 0 0 0
2	1	1	10	1	1	1	1	1	0.2197	1	-1	1	0 0 0 0
3	1	1	5	1	1	1	1	1	-0.437	-1	1	0 0 0 1	
4	1	1	5	1	1	1	1	1	-1	-0.7514	1	0 0 0 1	
5	1	1	10	1	1	1	1	1	0.1925	1	-1	1	0 0 0 0
6	1	5	5	10	5	0	4.6667	0	-0.3984	1	-1	1	0 0 0 0
7	1	5	5	1	5	0	8.3333	0	-1	1	-0.3511	1	0 0 0 0
8	1	5	5	1	5	0	7.625	0	0.0857	-1	1	1	0 0 0 0
9	1	5	5	1	5	1	1	1	1	-1	-0.5564	1	0 0 0 1
10	1	1	5	1	1	1	1	1	0.0692	1	-1	1	0 0 0 0
11	1	1	5	1	1	1	1	1	-0.3678	1	-1	1	0 0 0 0
12	1	1	5	1	1	1	1	1	-0.4813	1	-1	1	0 0 0 0
13	1	1	5	1	1	1	4.6667	0	-1	1	-0.5761	1	0 0 0 0
14	1	1	5	1	1	1	1	1	1	-1	-0.137	1	0 0 0 1
15	1	1	5	1	1	1	1	1	0.3601	-1	1	0	0 0 1
16	1	1	5	1	1	1	1	1	-1	1	-0.3002	1	0 0 0 0
17	5	5	5	10	5	1	3.2222	0	-1	1	-0.9872	0	1 0 0 1
18	5	5	5	1	5	1	1	0	-0.6839	1	-1	0	1 0 0 1
19	5	5	5	10	5	1	5	1	-1	1	-0.76	0	1 0 0 1
20	5	5	5	10	5	1	3.2222	1	-1	1	-0.7632	0	1 0 0 1
21	5	5	5	10	5	1	8.3333	0	-1	1	-0.7512	0	1 0 0 1
22	5	1	10	1	1	0	4.6667	1	1	-1	0.7744	0	1 0 0 0
23	5	5	5	1	5	1	5	1	-1	1	-0.7849	0	1 0 0 1
24	5	5	5	1	5	1	5	1	-0.3256	1	-1	0	1 0 0 1
25	5	5	5	1	5	1	4.6667	1	-1	1	-0.9202	0	1 0 0 1
26	5	1	5	1	1	0	1	0	0.4539	1	-1	0	1 0 0 1
27	5	1	5	1	1	0	1	0	1	-1	0.8684	0	1 0 0 0
28	10	5	10	10	10	1	10	1	-1	1	-0.6399	0	0 1 0 0
29	10	1	10	10	10	1	1	0	-0.77	-1	1	0	0 1 1 0
30	10	1	10	1	1	0	1	0	-1	1	-0.6625	0	0 1 0 0
31	10	5	10	10	10	1	3.2222	0	-0.7205	-1	1	0	0 1 1 1
32	10	5	10	10	10	1	10	1	-1	0.68	1	0	0 1 1 1
33	10	5	10	10	10	1	7.625	1	-1	1	0.5079	0	0 1 0 0
34	10	5	10	10	10	1	10	1	-1	1	-0.0761	0	0 1 0 0
35	10	5	10	10	10	1	1	0	1	-1	-0.4489	0	0 1 0 0
36	10	5	10	10	10	1	10	1	0.0498	-1	1	0	0 1 1 1
37	10	5	10	10	10	1	10	1	0.2217	-1	1	0	0 1 1 1
38	10	5	10	10	10	1	10	1	-0.3837	-1	1	0	0 1 1 1
Correct classification rate							31/38 =0.81 58		24/38 =0.6316				20/38 =0.5263

Table 5. Classification results of SVM, DT, and ANN using spectral data of 350 ~ 760 nm (Category 1-corn, Category 2-Dchinochloa crasgalli, and Category 3-Echinochloa crusgalli).

NO.	Real Value (1)	SVM Classification					DT Classification		ANN Classification					
		Cat. 1&2 (2)	Cat. 2&3 (3)	Cat. 1&3 (4)	Voting results (5)	True Judgement (6)	Results (7)	True Judgement (8)	Normolized results (9)			Real value (10)		True Judgement (11)
1	1	1	10	10	10	0	10	0	0.1997	1	-1	1	0	0
2	1	1	10	1	1	1	1	1	0.5307	1	-1	1	0	0
3	1	1	5	1	1	1	1	1	1	-1	0.6053	1	0	0
4	1	1	5	1	1	1	1	1	1	-1	-0.0809	1	0	0
5	1	1	10	1	1	1	1	1	1	-1	-0.7964	1	0	0
6	1	5	5	1	5	0	5	0	0.3741	1	-1	1	0	0
7	1	1	5	1	1	1	1	0	1	-1	-0.3289	1	0	0
8	1	1	5	1	1	1	10	0	-0.31	1	-1	1	0	0
9	1	1	5	1	1	1	1	1	0.0704	-1	1	0	0	1
10	1	1	5	1	1	1	1	1	-0.1581	-1	1	0	0	1
11	1	1	5	1	1	1	1	1	-1	-0.4111	1	0	0	1
12	1	1	5	1	1	1	3	1	1	-0.7395	-1	1	0	0
13	1	1	5	1	1	1	1	0	1	-0.0969	-1	1	0	0
14	1	1	5	1	1	1	1	1	-1	-0.2748	1	0	0	1
15	1	1	5	1	1	1	1.5714	1	1	-1	-0.3264	1	0	0
16	1	1	5	1	1	1	7.2857	1	1	-1	-0.6822	1	0	0
17	5	5	5	1	5	1	3.5	0	-0.9227	1	-1	0	1	0
18	5	5	5	1	5	1	1	0	-1	-0.5029	1	0	1	0
19	5	5	5	1	5	1	3.5	1	-0.8445	1	-1	0	1	0
20	5	1	5	10		0	3.5	1	-1	1	0.824	0	1	0
21	5	5	5	10	5	1	5	0	-0.9752	1	-1	0	1	0
22	5	1	10	1	1	0	1	1	0.0164	1	-1	0	1	0
23	5	5	5	1	5	1	5	1	-0.7423	1	-1	0	1	0
24	5	5	5	10	5	1	5	1	-0.2528	1	-1	0	1	0
25	5	5	5	1	5	1	5	1	-0.6211	1	-1	0	1	0
26	5	1	5	1	1	0	1.5714	0	0.6062	-1	1	0	1	0
27	5	1	10	1	1	0	1	0	0.3987	-1	1	0	1	0
28	10	1	10	10	10	1	10	1	-1	0.6507	1	0	0	1
29	10	1	10	10	10	1	3	0	-0.325	-1	1	0	0	1
30	10	1	10	10	10	1	10	0	0.463	1	-1	0	0	1
31	10	5	10	10	10	1	10	0	-0.7862	-1	1	0	0	1
32	10	5	10	10	10	1	10	1	-0.9069	-1	1	0	0	1
33	10	5	10	10	10	1	10	1	-1	-0.3425	1	0	0	1
34	10	5	10	10	10	1	1	1	-0.2053	-1	1	0	0	1
35	10	5	10	10	10	1	3.5	0	-0.2881	-1	1	0	0	1
36	10	5	10	10	10	1	1	1	-0.5917	-1	1	0	0	1
37	10	5	10	10	10	1	10	1	-0.8809	-1	1	0	0	1
38	10	5	10	10	10	1	10	1	-1	-0.7013	1	0	0	1
Correct classification rate		32/38 = 0.8421			26/38 = 0.6840								30/38 = 0.7890	

It is shown that the correct classification rates of SVM, DT, and ANN classifiers are 0.8158, 0.6316, and 0.5263, respectively, in the 350 ~ 2500 nm spectral range, and 0.8421, 0.6840, and 0.7890, respectively, in the 350 ~ 760 nm spectral wavelength range. Obviously, the overall correct classification rates obtained from the data of 350 ~ 760 nm wavelength range are even higher than those obtained from the data of 350 ~ 2500 nm. The results indicated that the narrower wavelength range in the visible spectrum is even more informative than the wider wavelength range in the visible and NIR spectrums, which could lead to the consideration of using visible spectra instead of VNIR spectra for weed detection. This would reduce the cost of optical sensors for weed management significantly.

4. Conclusions

The correct classification rates of three classifiers obtained from the data of 350 ~ 760 nm

wavelength range are higher than those obtained from the data of 350 ~ 2500 nm. Therefore, it could be unnecessary to take the entire VNIR spectral wavelength band as the spectral range for crop-weed discrimination. Instead, the visible light spectral range could be enough to meet the requirement of crop-weed spectral discrimination. This could result in reduced cost of weed detecting optical sensors.

Acknowledgements

This research was supported by the National High Technology Research and Development Program of China (863 Program) (No. 2012AA101904) and the National Sci-tech Support Plan Projects of China for the 12th five-year plan (2011BAD20B07). The authors acknowledge the National Experimental Station of Precision Agriculture of China.

References

- [1]. <http://www.fao.org/news/story/en/item/29402icode/>.
- [2]. J. Tang, Research on Weed Detection and Navigation Parameters Acquisition of Pesticide Spraying Robot, *North-west Agriculture and Forestry University*, Yang Ling, 2010.
- [3]. J. F. Thompson, J. V. Stafford, P. C. H. Miller, Potential for automatic weed detection and selective herbicide application, *Crop Protection*, Vol. 10, Issue 4, 1991, pp. 254-259.
- [4]. M. Molto, B. Martin, A. Gutierrez, Pesticide loss reduction by automatic adaptation of spraying on globular trees, *Journal of Agricultural Engineering Research*, Vol. 78, Issue 1, 2001, pp. 35-41.
- [5]. W. Wang, T. Hong, Y. Lu, et al., Performance of tree canopy diameter measurement based on ultrasonic sensor and DGPS, *Transactions of the Chinese Society of Agricultural Engineering*, Vol. 22, Issue 8, 2006, pp. 158-161.
- [6]. L. Anitori, A. Jong, F. Nennie, FMCW radar for life-sign detection, in *Proceedings of the IEEE Radar Conference*, Piscataway, 2009, pp. 1-6.
- [7]. W. Wang, M. Huang, Z. Bai, et al., Microwave-based sensor for detection of a shortage in tobacco box. in *Proceedings of the IEEE International Conference on Information Acquisition*, Piscataway, 2005, pp. 413-416.
- [8]. T. Bae, B. Kim, Y. Kim, et al., Small target detection using cross product based on temporal profile in infrared image sequences, *Computers & Electrical Engineering*, Vol. 36, Issue 6, 2010, pp. 1156-1164.
- [9]. J. Shaik, K. M. Iftekharuddin, Detection and tracking of targets in infrared images using Bayesian techniques, *Optics & Laser Technology*, Vol. 41, Issue 6, 2009, pp. 832-842.
- [10]. N. Wang, N. Zhang, F. E. Dowell, et al., Design of an optical weed sensor using plant spectral characteristics, *Transactions of the ASAE*, Vol. 44, Issue 2, 2001, pp. 409-419.
- [11]. A. Rogalski, Infrared detectors: status and trends, *Progress in Quantum Electronics*, Vol. 27, Issue 2, 2003, pp. 59-62.
- [12]. R. B. Brown, J. P. G. A. Steckler, and G. W. Anderson, Remote sensing for identification of weeds in no-till corn, *Transactions of the ASAE*, Vol. 37, Issue 1, 1994, pp. 297-302.
- [13]. E. Vriindts, J. D. Baerdemaeker, H. Ramon, Weed detection using canopy reflectance, in *Proceedings of the 2nd European Conference on Precision Agriculture*, 1999, pp. 257-264.
- [14]. T. Borregaard, H. Nielsen, L. Norgaard, et al., Crop Weed Discrimination by Line Imaging Spectroscopy, *Journal of Agricultural Engineering Research*, Vol. 75, Issue 4, 2000, pp. 389-400.
- [15]. M. J. Exposito, F. L. Granaries, S. Atenciano, et al., Discrimination of Weed Seedlings, Wheat (*Triticum aestivum*) Stubble and Sunflower (*Helianthus annuus*) by Near-Infrared Reflectance Spectroscopy (NIRS), *Crop Protection*, Issue 22, 2003, pp. 1177-1180.
- [16]. P. S. Thenkabail, E. A. Enclona, M. S. Ashton, et al., Accuracy Assessments of Hyperspectral Waveband Performance for Vegetation Analysis Applications. *Remote Sensing of Environment*, Issue 9, 2004, pp. 354-376.
- [17]. W. Mao, Y. Wang, Y. Wang, et al., Spectrum Analysis of Crop and Weeds at Seedling. *Spectroscopy and Spectral Analysis*, Vol. 25, Issue 6, 2005, pp. 984-987.
- [18]. D. Zhu, J. Pan, Y. He, Identification Methods of Crop and Weeds Based on Vis/NIR Spectroscopy and RBF-NN Model, *Spectroscopy and Spectral Analysis*, Vol. 28, Issue 5, 2008, pp. 1102-1106.
- [19]. W. Deng, L. Zhang, X. He, et al., SVM-Based Spectral Recognition of Corn and Weeds at Seedling Stage in Fields, *Spectroscopy and Spectral Analysis*, Vol. 29, Issue 7, 2009, pp. 1906-1910.
- [20]. S. Chen, Y. Li, H. Mao, et al., Research on Distinguishing Weed from Crop Using Spectrum Analysis Technology, *Spectroscopy and Spectral Analysis*, Vol. 29, Issue 2, 2009, pp. 463-466.
- [21]. B. Liu, J. Fang, X. Liu, et al., Research on Crop-Weed Discrimination Using a Field Imaging Spectrometer, *Spectroscopy and Spectral Analysis*, Vol. 30, Issue 7, 2010, pp. 1830-1833.
- [22]. Q. Zu, C. Zhao, W. Deng, et al., Research on discrimination of cabbage and weeds based on visible and near-infrared spectrum analysis, *Spectroscopy and Spectral Analysis*, Vol. 33, Issue 5, 2013, pp. 1202-1205.
- [23]. http://en.wikipedia.org/wiki/Support_vector_machine.
- [24]. S. Yang, Pattern Recognition & intelligent computation Matlab Tech, *Publishing House of Electronics Industry*, Beijing, 2008.
- [25]. J. Zhang, L. Zhang, M. Zang, et al., Prediction of Soybean Growth and Development Stages Using Artificial Neural Network and Statistical Models, *Acta Agronomica Sinica*, Vol. 35, Issue 2, 2009, pp. 341-347.
- [26]. G. Ramesh, P. Suranjan, and F. David, Neural network optimization of remotely sensed maize leaf nitrogen with a genetic algorithm and linear programming using five performance parameters, *Biosystems Engineering*, Vol. 95, Issue 3, 2006, pp. 359-370.
- [27]. D. John, J. Cai, Z. Cai, Decision Tree Technique and its Current Research, *Control Engineering of China*, Issue 1, 2005, pp. 15-18.
- [28]. I. H. Witten, E. Frank, Data Mining: Practical Machine Learning Tools and Techniques with Java Implementations, *Morgan Kaufmann Publishers*, Seattle, 2000, pp. 265-331.